

# Frame-Level Internal Tool Use for Temporal Grounding in Audio LMs

Joesh An<sup>1</sup> Phillip Keung<sup>1</sup> Jiaqi Wang<sup>1</sup> Orevaoghene Ahia<sup>1</sup> Noah A. Smith<sup>1,2</sup>

## Abstract

Large audio language models are increasingly used for complex audio understanding tasks, but they struggle with temporal tasks that require precise temporal grounding, such as word alignment and speaker diarization. The standard approach, where we generate timestamps as sequences of text tokens, is computationally expensive and prone to hallucination, especially when processing audio lengths outside the model’s training distribution. In this work, we propose *frame-level internal tool use*, a method that trains audio LMs to use their own internal audio representations to perform temporal grounding directly. We introduce a lightweight prediction mechanism trained via two objectives: a binary frame classifier and a novel inhomogeneous Poisson process (IHP) loss that models temporal event intensity. Across word localization, speaker diarization, and event localization tasks, our approach outperforms token-based baselines. Most notably, it achieves a  $>50\times$  inference speedup and demonstrates robust length generalization, maintaining high accuracy on out-of-distribution audio durations where standard token-based models collapse completely.

## 1. Introduction

Audio language models are now widely used for various audio understanding problems, especially temporal tasks that require grounding in the audio content (Goel et al., 2025; Ghosh et al., 2025; Team et al., 2023; KimiTeam et al., 2025; Xu et al., 2025b; Xie et al., 2025; Wijngaard et al., 2025). These tasks, such as word alignment to audio (McAuliffe et al., 2017b), speaker diarization (Anguera et al., 2007), and musical beat tracking (Dixon, 2000; 2007), require reference to precise timestamps in the audio. For example, in audio question answering, a question like ‘When did the dog start barking?’ may need to be answered in units

<sup>1</sup>University of Washington <sup>2</sup>Allen Institute for AI. Correspondence to: Joesh An <anjo0@cs.washington.edu>, Phillip Keung <pkeung@uw.edu>.

of milliseconds relative to the start of the input recording. Using an audio LM to produce timestamps is a natural goal, but the standard approach (where the LM generates timestamps as a sequence of text tokens) suffers from two notable and related problems.

Firstly, audio LMs are prone to hallucinations, as multi-modal LMs are typically constructed by coupling a modality-specific encoder with an LM decoder and have been observed to ignore the audio input in favor of the text prompt (Ahia et al., 2025; Sakshi et al., 2025). Because the text decoder is unconstrained, it can generate timestamps that are syntactically correct but have no correspondence to the audio content. Relatedly, audio LMs often memorize the text of the timestamps in the training data and struggle with *length generalization*, leading to large errors when predicting timestamps that fall outside of its training window (e.g., if all audio examples in training are less than  $n$  minutes long, then the model will not predict positions greater than  $n$  minutes). Because the decoder does not learn to map audio features to textual representations of time beyond its training distribution, the generated timestamps for these later segments are effectively ungrounded.

Secondly, text generation is ill-suited for a continuous task. It is computationally inefficient, replacing what should be a simple pointer to the audio sequence with an expensive auto-regressive process (e.g., generating 7–10 tokens for a single word-level timestamp for a range like ‘[2.39, 4.11]’). Also, this approach fails to use the rich temporal information already computed and internally aligned by the audio LM when processing the audio input.

The text-only approach stands in sharp contrast to the long history of models in speech recognition that use *frame-level objectives* (e.g., senone classification in DNN-HMM systems, Connectionist Temporal Classification (CTC); Graves et al., 2006, RNN-Transducer models; Graves, 2012). Concurrently, a separate line of research has developed LMs that are capable of tool use, enabling them to call external functions to augment their capabilities (Schick et al., 2023; Patil et al., 2024; Wang et al., 2025a; Hao et al., 2023). However, a major drawback of tool use is that it involves external models and API calls for different tasks, which imposes latency and maintenance costs.

We propose a new approach, *frame-level internal tool use*,

that bridges **frame-level temporal understanding** and **tool-augmented modeling** in audio LMs. Instead of forcing the audio LM to generate timestamps in text form, we train it to use an *internal* tool that operates directly on the model’s own representations. In our framework, the model learns to reuse its audio representations (including decoder outputs that are normally discarded, because they are not needed for token generation) to produce a probability distribution over audio frames for a given audio event query and to invoke external code to extract the relevant timestamps directly. The audio LM’s decoder, conditioned on a text prompt (e.g., “When did the second speaker start talking?”), learns to produce a frame-level alignment over its own audio representations. Simple, deterministic Python functions (e.g., peak detection, thresholding) are then applied to extract precise timestamps from this output distribution.

Our work draws inspiration from work on vision LMs like Molmo and HiMTok (Clark et al., 2026; Deitke et al., 2024; Wang et al., 2025b), where the model learns precise spatial and temporal grounding in visual inputs (images and videos). In Molmo, for example, the model is trained to generate pixel-level x-y coordinates and temporal indices corresponding to objects or events as part of its chain-of-thought and not through the use of external tools. In addition, recent work like ChronusOmni (Chen et al., 2025) also generates times and locations without external assistance, and uses an auxiliary reinforcement learning task to improve temporal grounding in video.

We explore two approaches to model the timestamps: 1) a discriminative binary loss for the frame where the audio event occurs, 2) modeling the time-varying intensity function for events in audio using an inhomogeneous Poisson process. Our experiments span three temporal tasks: i) word localization, ii) speaker diarization, and iii) audio event localization. Our key findings are as follows:

- Frame-level tool use improves both the accuracy and mean absolute deviation of predicted timestamps across all tasks compared to generating timestamps in text form. The Poisson-based loss generally outperforms the binary loss.
- Reusing audio representations is over 50 times faster than auto-regressive text generation, as it requires only a single parallel pass over the audio frames.
- In out-of-distribution scenarios, frame-level internal tool use substantially reduces hallucinated timestamps by grounding the model’s output directly in the audio frames rather than generating unconstrained text tokens.

In sum, our findings demonstrate that frame-level internal

tool use within audio LMs improves the accuracy and efficiency of fine-grained processing of audio content.

## 2. Frame-Level Internal Tool Use

Given the flexibility language models have shown for generating so many kinds of output, and given that timestamps referencing audio input can easily be represented as text symbols, it is natural to default to direct generation of timestamps as simply “more text” generated autoregressively. Our frame-level tool use approach instead learns to construct a probability distribution aligned with its own internal representations of the input audio. This section details the technical implementation of this mechanism.

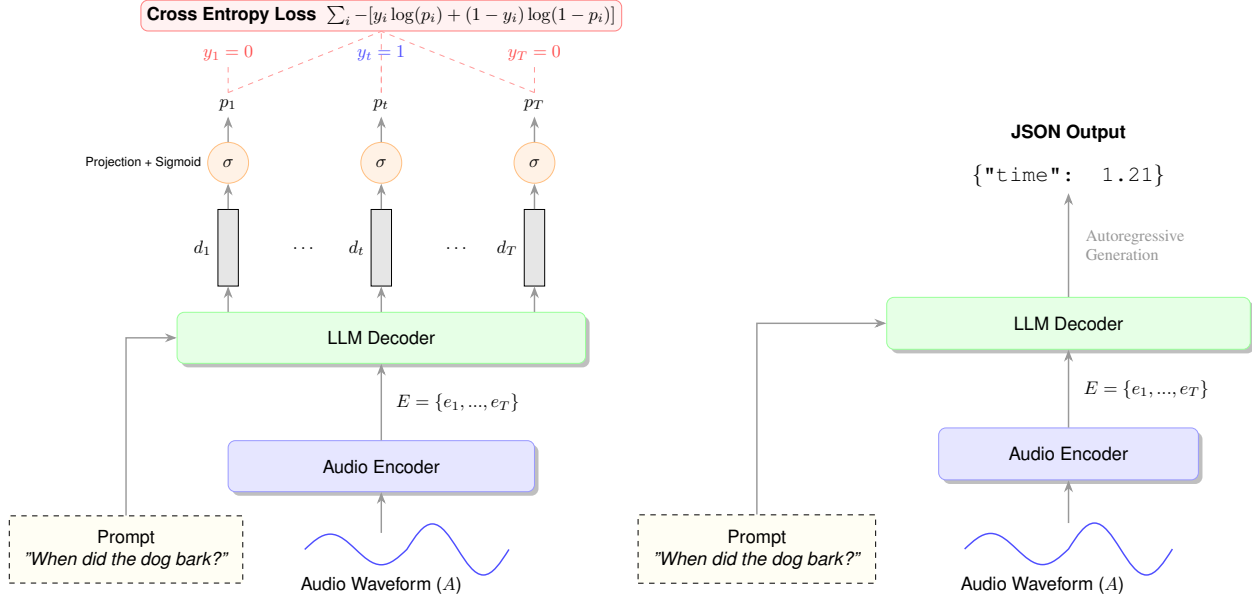
The LM’s audio representations,  $D = \{d_1, d_2, \dots, d_T\}$ , are conditioned on both the text prompt and the encoded input audio. We attach a lightweight prediction head to  $D$ . Using annotated data (described in §3), this head is trained to transform the decoder’s output states into a probability distribution over the temporal frames, where we interpret the probability assigned to frame  $t$  as the probability that the target event (referenced in the prompt) occurs at frame  $t$ . Simple, deterministic functions can then post-process this distribution to extract the final timestamps.

We explore two distinct frame-level loss functions, each making different assumptions about the temporal nature of the events. The first is a simple, reweighted binary cross-entropy loss, which treats each frame as an independent classification task (i.e., the frame where the event actually occurs in the training instance is a positive instance, and all the others are negative instances). The second loss function is a more structured loss derived from the theory of inhomogeneous Poisson processes, which models the continuous-time intensity of an event occurring. We present each in turn.

### 2.1. Binary Frame-Level Loss

In Figure 1, we illustrate binary frame-level tool use. We assume an audio LM architecture consisting of an audio encoder and a text-prompted decoder.

1. The audio encoder processes a raw audio waveform  $A$  into a sequence of audio feature representations,  $E = \{e_1, e_2, \dots, e_T\}$ , where  $T$  is the total number of frames.
2. The decoder, conditioned on a text prompt  $P$  (which describes the target event), ingests the encoder audio representations  $E$  to produce a sequence of decoder audio representations,  $D = \{d_1, d_2, \dots, d_T\}$ .  **$D$  refers to the outputs from the final layer of the decoder**, not the intermediate representations from any other layer.



(a) Binary frame-level tool training.  $E = \{e_1, \dots, e_T\}$  are the audio representations from the audio encoder, and  $\{d_1, \dots, d_T\}$  are the audio representations from the decoder's outputs.  $y_t = 1$  is the binary label where the event corresponding to the prompt occurred, all other labels are 0.

Figure 1. Frame-level prediction and generative output for predicting timestamps in audio. At inference time, we extract the predicted timestamp from the binary frame-level probabilities  $p_1, \dots, p_T$  via argmax.

Instead of using  $D$  to generate timestamps in text form, we attach a binary classification head (i.e., a parameter vector followed by a sigmoid activation) to each frame  $d_t$ . This head is trained to predict the probability  $p_t$  that frame  $t$  contains the target event. The ground truth for this task, during supervised training, is a binary sequence  $Y = \{y_1, y_2, \dots, y_T\}$ , where  $y_t = 1$  if the event described in  $P$  is present at frame  $t$ , and  $y_t = 0$  otherwise.

The usual binary cross-entropy loss for a single frame  $t$  of an audio recording is:

$$l_t = -[y_t \log(p_t) + (1 - y_t) \log(1 - p_t)] \quad (1)$$

where  $p_t$  is the model's predicted probability that  $y_t = 1$ .

Of course, most frames will have  $y_t = 0$ . We correct the resulting severe class imbalance by class reweighting. For example, for a frame rate of one frame per 40 ms of audio, a 30-second audio clip would be represented by 750 frames. However, the target events would only be present in a few frames. In the case of keyword spotting, the start and end of a word would be just 2 events out of 750 frames.

We use a class weight  $w$ , which is set to be equal to the ratio between the negative class frequency to the positive class frequency to ensure a balanced contribution to the total loss.

During inference, the model produces, as numerical (not textual) outputs, probabilities  $\{p_1, p_2, \dots, p_T\}$  for each 40

ms frame of audio. To extract  $k$  timestamps, we rank the probabilities for all frames in descending order and select the top- $k$  values. These indices correspond to the frames where the model has the highest confidence that the event described in the prompt  $P$  has occurred. The indices are converted into timestamps and then output textually. (For most common use cases such as extracting start-of-word timestamps from a transcript, the number of events  $k$  is known beforehand.)

## 2.2. Poisson Process Frame-level Loss

While the binary frame-level loss assumes that events are conditionally independent across time steps, events in audio often exhibit strong dependencies over time. Furthermore, binary classification requires tuning the class reweighting due to label imbalance and struggles with “fuzzy” or imprecise annotations. To address these limitations, we propose modeling event timestamps using an *inhomogeneous Poisson process* (IHP). This probabilistic framework naturally handles sparsity through intensity modeling and optimizes for the likelihood of the event sequence rather than making hard, independent decisions per frame.

## THE INHOMOGENEOUS POISSON PROCESS

The IHP is a stochastic counting process governing the occurrence of events over continuous time. The probability of an event occurring is defined by a time-varying intensity function, or *hazard rate*,  $\lambda(t) > 0$ . Loosely speaking,  $\lambda(t)$  is the (instantaneous) rate of events at time  $t$ .

We model the ground truth timestamps as the arrival times of such a process over the domain  $[0, T]$ , where  $T$  is the audio duration in frames.

## PARAMETERIZATION AND SPLINE CONSTRUCTION

We parameterize the event intensity  $\lambda(t)$  using the sequence of outputs from the audio LM’s decoder, denoted  $D = \{d_1, \dots, d_T\}$ . We project each frame-level representation  $d_k$  to a non-negative scalar rate  $\lambda_k$  via a learned projection head  $h$ :

$$\log \lambda_k = h^\top d_k \quad (2)$$

Figure 2 illustrates this parameterization in the simple case when  $n = 1$ , i.e., where we seek to determine the timestamp for a single event of interest, such as the start of a dog’s bark. The audio LM’s outputs over the audio frames are converted to scalars  $\log \lambda_i$  via the projection head.

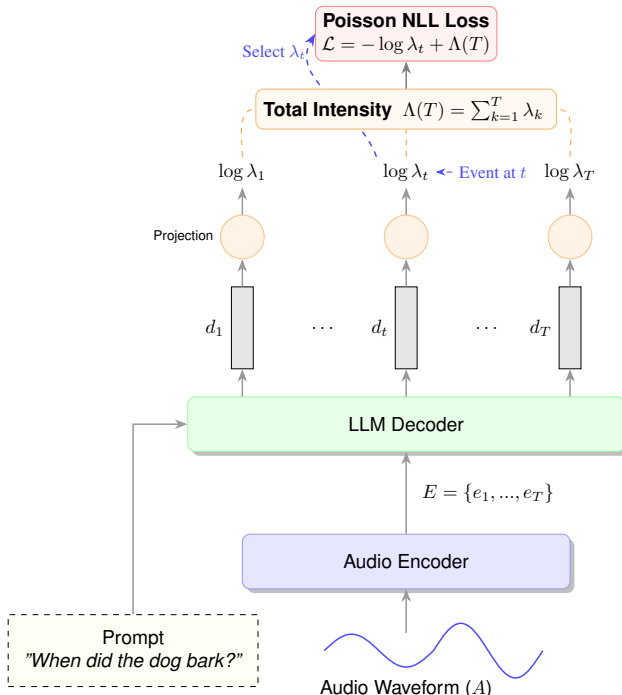


Figure 2. Inhomogeneous Poisson process frame-level tool training. In the simple case where only 1 timestamp is needed, the  $\log \lambda_1, \dots, \log \lambda_T$  are used to construct a non-parametric probability density estimator over the audio frames, normalized by the total intensity  $\Lambda(T) = \sum_{k=1}^T \lambda_k$ .

We model  $\lambda(t)$  as a piecewise constant spline:

$$\lambda(t) = \sum_{k=1}^T \lambda_k \mathbb{I}\{k-1 \leq t < k\} \quad (3)$$

Therefore, for any time  $t$  falling within the  $k$ -th frame, the instantaneous rate is exactly equal to  $\lambda_k$ .

When  $n = 1$ ,  $\lambda(t)$  is like an unnormalized energy function. To convert it into a valid probability distribution, we compute the normalizing constant, which corresponds to the cumulative energy over the entire audio duration. Since the energy function is a piecewise constant spline with knots at the end of each frame, the normalizing constant is the sum of the rates:  $\Lambda(T) = \int_0^T \lambda(t) dt = \sum_{i=1}^T \lambda_i$ . This summation is depicted in the “total intensity” (a.k.a, the cumulative hazard) in Figure 2.

In general, we define the cumulative intensity at time  $t$  to be  $\Lambda(t) = \int_0^t \lambda(t) dt$ . Note that  $\Lambda(t)$  is a continuous piecewise linear spline interpolating between the knots  $H_k = \sum_{j=1}^k \lambda_j$ , since  $\lambda(t)$  is itself a piecewise constant spline.

## LOSS FORMULATION

However, the number of events is not necessarily equal to 1. Consider a training instance with  $n$  event timestamps  $\mathbf{t} = \{t_1, \dots, t_n\}$  such that  $0 \leq t_1 \leq \dots \leq t_n \leq T$ . The probability density of observing exactly these arrival times under an IHP (Daley & Vere-Jones, 2006) is given by:

$$p(\mathbf{t} | n) = \frac{n! \prod_{i=1}^n \lambda(t_i)}{\Lambda(T)^n} \quad (4)$$

The negative log-likelihood loss for the sequence is therefore:

$$\mathcal{L} = - \sum_{j=1}^n \log \lambda(t_j) + n \log \Lambda(T) \quad (5)$$

In the single-event case ( $n = 1$ ) shown in Figure 2, this simplifies to  $\mathcal{L} = -\log \lambda_t + \Lambda(T)$ , where the model essentially learns to maximize the intensity at the target frame  $\lambda_t$  while suppressing the total energy  $\Lambda(T)$  elsewhere.

## INFERENCE

At inference time, given a predicted count of  $n$  events, we wish to extract timestamps  $\hat{t}_1, \dots, \hat{t}_n$ . The posterior mode corresponds to the most likely specific configuration of timestamps.

We begin with the *Time Rescaling Theorem* (Kingman, 1992), which maps the complex IHP to a homogeneous Poisson process.

**Theorem 2.1** (Time Rescaling). *If  $t_1, \dots, t_n$  is a realization of an IHP on  $[0, T]$  with cumulative hazard  $\Lambda(t)$ , then*

the transformed values  $z_i = \Lambda(t_i)$  form a unit-rate homogeneous Poisson process on the interval  $[0, \Lambda(T)]$ .

Conditioned on observing  $n$  events, the sorted transformed timestamps  $z_{(1)} < \dots < z_{(n)}$  are distributed as the order statistics of  $n$  independent  $\text{Uniform}(0, \Lambda(T))$  variables. The  $i$ th ordered variable  $z_{(i)}$  follows a scaled Beta distribution with parameters  $\alpha = i$  and  $\beta = n + 1 - i$ :

$$p_Z(z) \propto z^{i-1} (\Lambda(T) - z)^{n-i} \quad \text{for } z \in [0, \Lambda(T)] \quad (6)$$

We perform an appropriate change of variables to recover the posterior mode in the original time domain. Let  $t$  denote the random variable for the  $i$ th timestamp in the original domain. The mapping is defined by  $z = \Lambda(t)$ . The probability density function  $p_T(t)$  is related to  $p_Z(z)$  by the Jacobian of the transformation:

$$p_T(t) = p_Z(\Lambda(t)) \cdot \left| \frac{d}{dt} \Lambda(t) \right| \quad (7)$$

Recalling that the derivative of the cumulative hazard is the intensity function itself, i.e.,  $\frac{d}{dt} \Lambda(t) = \lambda(t)$ , we obtain the density for the  $i$ -th timestamp:

$$p_T(t) \propto \underbrace{\Lambda(t)^{i-1} (\Lambda(T) - \Lambda(t))^{n-i}}_{\text{Beta contribution}} \cdot \underbrace{\lambda(t)}_{\text{Jacobian}} \quad (8)$$

The posterior mode  $\hat{t}_i$  is the time  $t$  that maximizes this density. Taking the logarithm, we find the timestamp to be  $\hat{t}_i = \arg \max_{t \in [0, T]} \log p_T(t)$ . Since  $\lambda(t)$  is a piecewise constant spline,  $\Lambda(t)$  is monotonically increasing, and the beta density function is unimodal,  $\log p_T(t)$  can be maximized very efficiently by evaluating it at the spline knots for each frame and at the beta mode.

### 3. Experimental Setup

#### 3.1. Task and Datasets

Our experiments focus on improving audio LMs’ performance on human speech understanding across three tasks: (i) word localization, (ii) speaker diarization, and (iii) audio event localization. We describe the datasets used for these experiments below.

**Word Localization:** We train and test on the LibriSpeech train-clean-100, dev-clean, and test-clean datasets (Panayotov et al., 2015). Ground truth timestamps are extracted using the Montreal Forced Aligner (McAuliffe et al., 2017a) via forced alignment. Each audio recording includes the transcript and the start and end timestamps for each word.

**Speaker Diarization:** We use the LibriCount dataset (Stöter et al., 2019), a synthetic “cocktail party” dataset. In this setting, the task is to predict the start time of each unique

speaker in a recording. Each recording contains between 1 and 10 speakers, with start times annotated for all.

**Audio Event Localization:** For identifying timestamps of audio events in the wild, we use the human sounds subset of the AudioSet dataset (Gemmeke et al., 2017). AudioSet consists of 10-second clips from YouTube, each annotated with one or more sound categories. We focus on the strongly-labeled portion, where each acoustic event in a recording is annotated with precise start and end times.

#### 3.2. Modeling

We conducted a series of experiments to validate the effectiveness of frame-level tool use for temporal grounding in audio LMs. First, we evaluate a range of open-weight audio LMs—Audio Flamingo 3 (Goel et al., 2025), Voxtral (Liu et al., 2025), and Qwen2.5-Omni (Xu et al., 2025a)—as well as proprietary audio LMs, including Gemini 2.5 Flash (Team et al., 2023) and GPT-4o (OpenAI et al., 2024), in zero-shot setting across all tasks described in §3. This is to establish a state-of-the-art baseline performance for these tasks that rely on text-based timestamp generation.

Next, we finetune Qwen2.5-Omni 3B and 7B models on all tasks using the same datasets, training them to perform frame-level tool use with the binary and Poisson-based frame losses described in §2.1 and §2.2. We compared these models against text token-based timestamp generation baselines, which are fine-tuned using the same Qwen models under identical training conditions. We used compute nodes with 4 Nvidia H100 GPUs for training and inference. Hyperparameters are provided in the Appendix.

#### 3.3. Evaluation Metrics

We evaluate the quality of generated timestamps with *frame-level accuracy* (whether predicted timestamp falls within 100 ms of the ground truth) and *mean absolute deviation* (MAD). For binary frame-level loss, the middle of the chosen frame is taken as the predicted timestamp.

### 4. Results and Discussion

We present quantitative results evaluating frame-level tool use across multiple audio tasks, covering several aspects of model performance discussed below. We describe each experiment and our respective findings.

#### 4.1. Can Audio LMs Predict Timestamps Zero-Shot?

In Table 1, we present the zero-shot accuracies and mean absolute deviations across our tasks. In this setting, models are prompted to directly generate timestamps in text form without any task-specific fine-tuning. Overall, zero-shot performance is poor across all benchmarks, indicating that

Table 1. Zero-shot performance of audio LMs on temporal tasks. We report accuracies (%) at different tolerances (20ms, 40ms, 100ms) and mean absolute deviation (MAD, seconds). Models are prompted to generate timestamps directly from audio without task-specific fine-tuning. Results show that all models struggle in this zero-shot setting, with low accuracy and high MAD across tasks.

Model	LibriSpeech (Word Align.)			LibriCount (Speaker Diar.)			AudioSet (Human Vocal.)		
	20ms ↑	40ms ↑	MAD ↓	40ms ↑	100ms ↑	MAD ↓	40ms ↑	100ms ↑	MAD ↓
Audio Flamingo 3	0.6%	1.4%	1.82	<b>2.3%</b>	<b>6.3%</b>	<b>1.53</b>	5.8%	10.2%	<b>1.69</b>
Voxtral 3B	0.8%	1.1%	2.52	0.3%	1.2%	6.02	1.2%	2.2%	3.74
Voxtral 24B	0.2%	0.5%	2.12	0.4%	1.4%	4.91	2.3%	4.2%	4.03
Qwen2.5 3B	0.1%	0.2%	2.59	0.6%	1.9%	3.71	3.6%	4.5%	4.46
Qwen2.5 7B	0.7%	1.1%	2.17	0.4%	1.5%	5.29	3.9%	5.7%	3.52
Gemini 2.5 Flash	<b>7.7%</b>	<b>13.8%</b>	<b>0.28</b>	1.1%	2.3%	2.69	<b>6.6%</b>	<b>12.7%</b>	2.30
GPT-4o Audio	0.3%	0.5%	2.42	0.2%	1.1%	4.60	1.9%	2.8%	3.80

current audio language models struggle to perform timestamp generation tasks accurately. Gemini 2.5 Flash achieves the highest overall performance; however, its average accuracy across tasks remains low.

#### 4.2. Fine-Tuning Audio LMs with Frame-Level Tool Use

In section §4.1, we show that audio LMs perform poorly at generating timestamps in the zero-shot setting. Our goal is to improve this performance using frame-level tool use, which grounds predictions directly in the model’s internal audio representations rather than relying on unconstrained text generation. A valid concern is that low performance could simply be due to a lack of task-specific training data. To test this, we directly fine-tune Qwen2.5-Omni to generate timestamps using the standard token-based approach. We consider this a useful baseline, as it allows us to isolate the benefits of frame-level tool use. This token-based fine-tuning serves as a strong baseline against which we compare our frame-level tool use methods.

Next, we fine-tune Qwen2.5-Omni 3B and 7B models on all tasks using frame-level tool use with both binary loss (§2.1) and the Poisson loss (§2.2). Table 2 summarizes the accuracies and mean absolute deviations (MADs) across tasks. Since all three methods achieve near-perfect accuracies at the 100ms threshold on LibriSpeech, we report 20ms accuracies to highlight differences between the methods. Across all tasks and both model sizes, the Poisson frame-level loss consistently outperforms token-based generation and binary frame-level loss, achieving the highest accuracies and lowest MADs on LibriSpeech, LibriCount, and AudioSet.

#### 4.3. Generalizing to Multiple Timestamp Generation

Our earlier experiments focused on predicting timestamps for single events, so we next investigate whether the Poisson frame-level loss can generalize to multiple timestamps. We finetune Qwen 2.5-Omni 7B separately on the word localization task using either token-based timestamp generation or Poisson frame-level loss, but with targets modified to

include timestamps for all words in each transcript rather than a single randomly selected word.

We report results on full data and across transcript-length buckets in Table 3 (longer transcripts contain more words, requiring more timestamp predictions). Overall, Poisson frame-level inference maintains performance comparable to classical token-based inference while providing substantial speedups, even as batch size increases. We provide further discussion on these efficiency gains in the next section.

#### 4.4. Frame-Level Tool Use Enables Efficient Generation

The primary drawback of timestamp generation with audio LMs is the computational cost of autoregressive decoding; each timestamp is generated sequentially, and each new token requires reprocessing all previously generated tokens. This leads to rapidly increasing inference time as the number of timestamps to be predicted grows. Frame-level tool use avoids autoregressive decoding altogether. Audio is processed once, in parallel, and timestamps are inferred directly from frame-level predictions without additional forward passes through the model.

To quantify the efficiency gains, we compare wall-clock inference time for generating multiple timestamps using token-based generation versus Poisson-based frame-level inference, as shown in Figure 3. We bucket examples by transcript length to analyze how runtime scales with the number of timestamps produced, as longer transcripts generally require predicting more timestamps. We observe a substantial speedup when generating timestamps using Poisson-based frame-level inference, especially when the number of words in the transcript is high. Across smaller batch sizes, inference is consistently faster than token-based generation, while at larger batch sizes we measure up to a  $\sim 5\times$  speedup after averaging wall-clock times over the buckets.

Table 2. Finetuned accuracies (Acc, %) and MAD (s) for Qwen audio LLMs with and without frame-level tool use. Highest accuracies and lowest MADs are bolded. Models tuned with Poisson loss outperform models tuned with either token or binary loss.

Model	Method	LibriSpeech			LibriCount			AudioSet		
		20ms ↑	40ms ↑	MAD ↓	40ms ↑	100ms ↑	MAD ↓	40ms ↑	100ms ↑	MAD ↓
Qwen2.5.3B	Tokens	91.4%	96.0%	0.08	60.8%	73.2%	<b>0.13</b>	40.9%	55.1%	1.15
	Poisson	<b>93.8%</b>	<b>97.9%</b>	<b>0.01</b>	<b>64.8%</b>	<b>75.2%</b>	<b>0.13</b>	<b>41.0%</b>	<b>59.3%</b>	<b>1.02</b>
	Binary	85.8%	96.1%	0.02	58.4%	72.0%	0.17	<b>41.0%</b>	57.7%	1.08
Qwen2.5.7B	Tokens	93.2%	97.1%	0.03	62.1%	75.3%	0.13	40.1%	56.9%	1.03
	Poisson	<b>93.3%</b>	<b>98.1%</b>	<b>0.01</b>	<b>65.9%</b>	<b>76.5%</b>	<b>0.12</b>	<b>42.3%</b>	<b>58.5%</b>	<b>0.99</b>
	Binary	85.7%	96.5%	0.03	63.6%	75.5%	0.13	40.6%	55.8%	1.14

Table 3. Qwen2.5-Omni 7B performance on predicting start-of-word timestamps in LibriSpeech, stratified by number of words in the transcript. Training with either the token or Poisson loss result in very similar performance.

# of Words	Tokens-only			Poisson		
	20ms ↑	40ms ↑	MAD ↓	20ms ↑	40ms ↑	MAD ↓
1-5	<b>94.6%</b>	<b>98.1%</b>	<b>0.01</b>	94.0%	97.4%	<b>0.01</b>
6-10	94.2%	97.3%	<b>0.01</b>	<b>94.9%</b>	<b>97.8%</b>	<b>0.01</b>
11-15	94.7%	97.8%	<b>0.01</b>	<b>95.3%</b>	<b>98.1%</b>	<b>0.01</b>
16-20	94.3%	<b>97.3%</b>	<b>0.01</b>	<b>94.5%</b>	97.1%	<b>0.01</b>
21-25	<b>94.5%</b>	<b>97.6%</b>	<b>0.01</b>	94.4%	97.3%	<b>0.01</b>
26+	<b>92.0%</b>	<b>94.9%</b>	0.11	91.6%	94.2%	<b>0.02</b>
	<b>93.2%</b>	<b>96.2%</b>	0.06	93.1%	95.8%	<b>0.02</b>

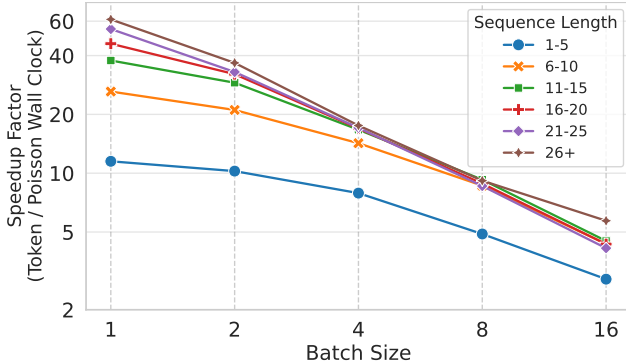


Figure 3. Speed-up factor between token-based and Poisson-based timestamp generation across batch sizes. Efficiency gains are larger when the timestamp sequences are long. Poisson-based timestamps are as much 60× faster than token-based timestamps.

#### 4.5. Frame-Level Tool Use Generalizes to Out-of-Distribution Timestamps

Accurately predicting timestamps for audio events beyond the range observed during training is important for real world applications. It is known that audio LLMs are prone to memorization and hallucinations (Kuan & Lee, 2025; Ahia et al., 2025) so they may produce timestamps that reflect patterns seen in their training data rather than the actual audio content during inference. To investigate this, we finetune Qwen2.5-Omni on progressively larger timestamp ranges—from 0–4 seconds up to 0–20 seconds—using Token loss, Poisson frame-level loss, or Binary frame-level loss and evaluate accuracy and MAD on timestamps outside the range seen during training.

As shown in Table 4, models trained with token loss perform well on in-distribution timestamps but fail to generalize to out-of-distribution timestamps, with high variability in performance. In contrast, our frame-level losses are much more robust: although out-of-distribution performance is slightly lower than in-distribution performance, the Poisson frame-level loss consistently achieves the highest accuracy and lowest MAD, outperforming both binary frame-level and token-based losses. These results suggest that grounding predictions in their audio representations, rather than relying on sequential token generation, allows the model to generalize more effectively to timestamps beyond the training range.

#### 4.6. Interpolating Token and Poisson Loss

We further investigate whether combining the token-based and Poisson frame-level loss can provide complementary benefits to model performance. The intuition is that encouraging the model to generate text tokens alongside frame-level predictions might provide additional guidance for learning precise timestamps. To test this, we implemented a training regimen that adds the two losses together, weighted by a tunable coefficient  $\lambda$ , i.e.,  $L = T + \lambda P$ , where  $T$  is the token loss and  $P$  is the Poisson frame-level loss. We ran experiments with  $\lambda = 0.05$  (other values such as 0.01 and 1.0 showed similar results) and report the results in Table 5. Overall we find that interpolating token and Poisson losses does not consistently improve performance over using the Poisson frame-level loss alone.

## 5. Related Work

**Point Processes in Machine Learning** Point processes have been applied in various problems to model the occurrence of events in time and space across diverse settings (e.g., earthquakes, cosmology, insurance, etc.); see the treatise by Daley & Vere-Jones (2006) for a survey. Mei & Eisner (2017) incorporated point processes like the Hawkes process into recurrent neural networks to model the arrival times of events in medical, social media, and financial data. Huang et al. (2019) incorporate a latent recurrent Poisson process model in an RNN-HMM speech recognition system to account for the occurrence time of senones. The latent

Table 4. Librispeech word alignment accuracies and mean absolute deviation (MAD) under matched (e.g., train on timestamps between 0-8 seconds and test on timestamps that are between 0-8 seconds) and mismatched (e.g., train on 0-8 seconds but test on 8-12 seconds) settings. The Poisson loss generalizes to out-of-distribution timestamps, whereas the token loss does not.

Train	Test	Tokens-only			Poisson			Binary		
		20ms ↑	40ms ↑	MAD ↓	20ms ↑	40ms ↑	MAD ↓	20ms ↑	40ms ↑	MAD ↓
<i>Matched Distributions</i>										
0-4s	0-4s	93.5%	97.5%	0.01	94.1%	98.0%	0.01	85.4%	96.3%	0.03
0-8s	0-8s	93.7%	97.6%	0.01	93.9%	98.1%	0.01	88.2%	96.9%	0.02
0-12s	0-12s	93.5%	97.8%	0.01	94.1%	98.3%	0.01	86.6%	95.9%	0.03
0-16s	0-16s	93.7%	97.9%	0.01	93.9%	98.4%	0.01	85.3%	96.2%	0.04
0-20s	0-20s	92.0%	96.2%	0.05	93.9%	98.1%	0.01	86.1%	96.3%	0.05
<i>Mismatched Distributions</i>										
0-4s	4-8s	0.9%	1.5%	2.35	92.3%	97.3%	0.03	83.5%	94.3%	0.14
0-8s	8-12s	3.3%	3.6%	2.32	94.0%	97.8%	0.03	86.7%	96.3%	0.09
0-12s	12-16s	7.4%	8.5%	2.00	91.2%	96.6%	0.04	81.0%	91.5%	0.20
0-16s	16-20s	0.0%	0.0%	2.40	94.2%	98.1%	0.07	84.6%	95.5%	0.31
0-20s	20+s	27.0%	28.6%	3.06	85.7%	95.2%	0.01	71.4%	87.3%	0.49

Table 5. Comparison of model performance between using only token loss, Poisson loss, and an interpolation of the two losses. We ran all of our experiments with  $L_{\text{interpolated}} = L_{\text{tokens}} + 0.05L_{\text{Poisson}}$ . Interpolating the two losses shows no consistent improvement on token outputs.

	Librispeech			Libricount			AudioSet		
	20ms ↑	40ms ↑	MAD ↓	40ms ↑	100ms ↑	MAD ↓	40ms ↑	100ms ↑	MAD ↓
Tokens-only	91.4%	96.0%	0.08	60.8%	73.2%	0.13	40.9%	55.1%	1.15
Poisson	93.8%	97.9%	0.01	64.8%	75.2%	0.13	41.0%	59.3%	1.02
<i>Interpolated loss with Poisson frame-level loss and token loss</i>									
Token Output	92.2%	96.4%	0.06	62.8%	72.7%	0.15	41.2%	57.5%	1.01
Poisson Output	94.2%	98.1%	0.01	63.7%	74.0%	0.15	41.3%	58.5%	1.04

process attempts to compensate for errors in the timing of the labels due to discretization and forced alignment. To the best of our knowledge, we are the first to apply point processes to temporal tasks with audio LMs.

**Internal Tool Use in Multimodal LMs** We have also observed a trend towards internal tool use in recent publications on multimodal models. Wang et al. (2025b) generates image segmentation masks as tokens using a vision LM and a hierarchical mask loss. Deitke et al. (2024); Clark et al. (2026) generate `<POINT>` tags and x-y co-ordinates to refer to relevant objects as part of the chain-of-thought and the final answer.

**Temporal Grounding in Multimodal LMs** Li et al. (2022) introduced a variant on the usual cross attention mechanism of a CNN-LSTM encoder-decoder model to jointly align the query with the audio and visual features in videos for question answering. GroundingGPT (Li et al., 2024) is one of the earlier works that pretrained and finetuned a multimodal LM with spatial and temporal tasks in mind, but the grounding was limited to producing timestamps and co-ordinates in token form. ChronusOmni and Time-R1 (Chen et al., 2025; Wang et al., 2025c) also generated timestamps in token form for moment retrieval in videos and applied reinforcement learning with interval over-

lap as the reward function to strengthen temporal grounding. We depart from these approaches by reusing existing internal representations of the audio LM for grounding instead of generating tokens directly.

## 6. Conclusion

We present *frame-level internal tool use*, a method that trains audio LLMs to leverage their internal audio representations for direct temporal grounding across multiple temporal understanding tasks, including word-level alignment, and speaker diarization and audio event localization. By predicting timestamps over audio frames rather than autoregressively generating them as text tokens, our approach improves timestamp prediction accuracy across all tasks. Extensive experiments in the paper demonstrate that our Poisson-based frame-level losses consistently outperform token-based generation baselines, maintaining high accuracy across both in-distribution and out-of-distribution audio sequences. We also show that our method provides substantial computational speedups, achieving over 50× faster inference compared to autoregressive token-based timestamp generation. Overall, frame-level internal tool use offers an efficient and effective approach for improving temporal grounding in audio LMs.

## References

Ahia, O., Bartelds, M., Ahuja, K., Gonen, H., Hofmann, V., Arora, S., Li, S. S., Puttagunta, V., Adeyemi, M., Buchireddy, C., Walls, B., Bennett, N., Watanabe, S., Smith, N. A., Tsvetkov, Y., and Kumar, S. Blab: Brutally long audio bench, 2025. URL <https://arxiv.org/abs/2505.03054>.

Anguera, X., Bozonnet, S., Evans, N., Fredouille, C., Friedland, G., and Vinyals, O. Speaker diarization: A review of recent research. *IEEE/ACM Transactions on Audio, Speech, and Language Processing*, 15(7):1412–1421, 2007. Survey of classical and early diarization systems.

Chen, Y., Wu, Y., Guan, K., Ren, Y., Wang, Y., Song, R., and Ru, L. Chronusomni: Improving time awareness of omni large language models. *ArXiv*, abs/2512.09841, 2025. URL <https://api.semanticscholar.org/CorpusID:283721592>.

Clark, C., Zhang, J., Ma, Z., Park, J. S., Salehi, M., Tripathi, R., Lee, S., Ren, Z., Kim, C. D., Yang, Y., Shao, V., Yang, Y., Huang, W., Gao, Z., Anderson, T., Zhang, J., Jain, J., Stoica, G., Han, W., Farhadi, A., and Krishna, R. Molmo2: Open weights and data for vision-language models with video understanding and grounding, 2026. URL <https://arxiv.org/abs/2601.10611>.

Daley, D. and Vere-Jones, D. *An Introduction to the Theory of Point Processes: Volume I: Elementary Theory and Methods*. Probability and Its Applications. Springer New York, 2006. ISBN 9780387215648. URL <https://books.google.com/books?id=6Sv4BwAAQBAJ>.

Deitke, M., Clark, C., Lee, S., Tripathi, R., Yang, Y., Park, J. S., Salehi, M., Muennighoff, N., Lo, K., Soldaini, L., Lu, J., Anderson, T., Bransom, E., Ehsani, K., Ngo, H., Chen, Y., Patel, A., Yatskar, M., Callison-Burch, C., Head, A., Hendrix, R., Bastani, F., VanderBilt, E., Lambert, N., Chou, Y., Chheda, A., Sparks, J., Skjonsberg, S., Schmitz, M., Sarnat, A., Bischoff, B., Walsh, P., Newell, C., Wolters, P., Gupta, T., Zeng, K.-H., Borchardt, J., Groeneveld, D., Nam, C., Lebrecht, S., Wittlif, C., Schoenick, C., Michel, O., Krishna, R., Weihls, L., Smith, N. A., Hajishirzi, H., Girshick, R., Farhadi, A., and Kembhavi, A. Molmo and pixmo: Open weights and open data for state-of-the-art vision-language models, 2024. URL <https://arxiv.org/abs/2409.17146>.

Dixon, S. A beat tracking system for audio signals. In *Proceedings of the ICMC*, 2000. OFAI-TR-2000-06.

Dixon, S. Evaluation of the audio beat tracking system BeatRoot. *Journal of New Music Research*, 36(1):39–58, 2007.

Gemmeke, J. F., Ellis, D. P. W., Freedman, D., Jansen, A., Lawrence, W., Moore, R. C., Plakal, M., and Ritter, M. Audio set: An ontology and human-labeled dataset for audio events. In *Proc. IEEE ICASSP 2017*, New Orleans, LA, 2017.

Ghosh, S., Kong, Z., Kumar, S., Sakshi, S., Kim, J., Ping, W., Valle, R., Manocha, D., and Catanzaro, B. Audio flamingo 2: An audio-language model with long-audio understanding and expert reasoning abilities. In *Forty-second International Conference on Machine Learning*, 2025. URL <https://openreview.net/forum?id=xWu5qpDK6U>.

Goel, A., Ghosh, S., Kim, J., Kumar, S., Kong, Z., Lee, S.-g., Yang, C.-H. H., Duraiswami, R., Manocha, D., Valle, R., and Catanzaro, B. Audio flamingo 3: Advancing audio intelligence with fully open large audio language models. *arXiv preprint arXiv*, 2025.

Graves, A. Sequence transduction with recurrent neural networks, 2012. URL <https://arxiv.org/abs/1211.3711>.

Graves, A., Fernández, S., Gomez, F., and Schmidhuber, J. Connectionist temporal classification: labelling unsegmented sequence data with recurrent neural networks. In *Proceedings of the 23rd International Conference on Machine Learning*, ICML '06, pp. 369–376, New York, NY, USA, 2006. Association for Computing Machinery. ISBN 1595933832. doi: 10.1145/1143844.1143891. URL <https://doi.org/10.1145/1143844.1143891>.

Hao, S., Liu, T., Wang, Z., and Hu, Z. ToolkenGPT: Augmenting frozen language models with massive tools via tool embeddings. In *Thirty-seventh Conference on Neural Information Processing Systems*, 2023. URL <https://openreview.net/forum?id=BHXsb69bSx>.

Huang, H., Wang, H., and Mak, B. Recurrent poisson process unit for speech recognition. In *Proceedings of the Thirty-Third AAAI Conference on Artificial Intelligence and Thirty-First Innovative Applications of Artificial Intelligence Conference and Ninth AAAI Symposium on Educational Advances in Artificial Intelligence*, AAAI'19/IAAI'19/EAAI'19. AAAI Press, 2019. ISBN 978-1-57735-809-1. doi: 10.1609/aaai.v33i01.33016538. URL <https://doi.org/10.1609/aaai.v33i01.33016538>.

KimiTeam, Ding, D., Ju, Z., Leng, Y., Liu, S., Liu, T., Shang, Z., Shen, K., Song, W., Tan, X., Tang, H., Wang, Z., Wei, C., Xin, Y., Xu, X., Yu, J., Zhang, Y., Zhou, X., Charles, Y., Chen, J., Chen, Y., Du, Y., He, W., Hu, Z., Lai, G., Li, Q., Liu, Y., Sun, W., Wang, J., Wang, Y., Wu, Y., Wu, Y., Yang, D., Yang, H., Yang, Y., Yang, Z., Yin, A., Yuan,

R., Zhang, Y., and Zhou, Z. Kimi-audio technical report. *arXiv preprint arXiv:2504.18425*, 2025.

Kingman, J. *Poisson Processes*. Oxford Studies in Probability. Clarendon Press, 1992. ISBN 9780191591242. URL <https://books.google.com/books?id=VEiM-OtwDHkC>.

Kuan, C.-Y. and Lee, H.-Y. Can large audio-language models truly hear? tackling hallucinations with multi-task assessment and stepwise audio reasoning. In *ICASSP 2025 - 2025 IEEE International Conference on Acoustics, Speech and Signal Processing (ICASSP)*, pp. 1–5, 2025. doi: 10.1109/ICASSP49660.2025.10888384.

Li, G., Wei, Y., Tian, Y., Xu, C., rong Wen, J., and Hu, D. Learning to answer questions in dynamic audio-visual scenarios. *2022 IEEE/CVF Conference on Computer Vision and Pattern Recognition (CVPR)*, pp. 19086–19096, 2022. URL <https://api.semanticscholar.org/CorpusID:247763132>.

Li, Z., Xu, Q., Zhang, D., Song, H., Cai, Y., Qi, Q., Zhou, R., Pan, J., Li, Z., Vu, V. T., Huang, Z., and Wang, T. Groundinggpt:language enhanced multi-modal grounding model. *ArXiv*, abs/2401.06071, 2024. URL <https://api.semanticscholar.org/CorpusID:266933314>.

Liu, A. H., Ehrenberg, A., Lo, A., Denoix, C., Barreau, C., Lample, G., Delignon, J.-M., Chandu, K. R., von Platen, P., Muddireddy, P. R., Gandhi, S., Ghosh, S., Mishra, S., Foubert, T., Rastogi, A., Yang, A., Jiang, A. Q., Sablayrolles, A., Héliou, A., Martin, A., Agarwal, A., Roux, A., Darzet, A., Mensch, A., Bout, B., Rozière, B., Monicault, B. D., Bamford, C., Wallenwein, C., Renaudin, C., Lanfranchi, C., Dabert, D., Chaplot, D. S., Mizelle, D., de las Casas, D., Chane-Sane, E., Fugier, E., Hanna, E. B., Berrada, G., Delerce, G., Guinet, G., Novikov, G., Martin, G., Jaju, H., Ludziejewski, J., Rute, J., Chabran, J.-H., Chudnovsky, J., Studnia, J., Barmentlo, J., Amar, J., Roberts, J. S., Denize, J., Saxena, K., Yadav, K., Khandelwal, K., Jain, K., Lavaud, L. R., Blier, L., Zhao, L., Martin, L., Saulnier, L., Gao, L., Pellat, M., Guillaumin, M., Felardos, M., Dinot, M., Darrin, M., Augustin, M., Seznec, M., Gupta, N., Raghuraman, N., Duchenne, O., Wang, P., Saffer, P., Jacob, P., Wambergue, P., Kurylowicz, P., Chagniot, P., Stock, P., Agrawal, P., Delacourt, R., Sauvestre, R., Soletskyi, R., Vaze, S., Subramanian, S., Garg, S., Dalal, S., Gandhi, S., Aithal, S., Antoniak, S., Scao, T. L., Schueller, T., Lavril, T., Robert, T., Wang, T., Lacroix, T., Bewley, T., Nemchikova, V., Paltz, V., Richard, V., Li, W.-D., Marshall, W., Zhang, X., Wan, Y., and Tang, Y. Voxtral, 2025. URL <https://arxiv.org/abs/2507.13264>.

McAuliffe, M., Socolof, M., Mihuc, S., Wagner, M., and Sonderegger, M. Montreal forced aligner: Trainable text-speech alignment using kaldi. In *Interspeech*, 2017a. URL <https://api.semanticscholar.org/CorpusID:12418404>.

McAuliffe, M., Socolof, M., Mihuc, S., Wagner, M., and Sonderegger, M. Montreal Forced Aligner: Trainable Text-Speech Alignment Using Kaldi. In *Proc. Interspeech 2017*, pp. 498–502, 2017b. doi: 10.21437/Interspeech.2017-1386.

Mei, H. and Eisner, J. The neural hawkes process: A neurally self-modulating multivariate point process. In *unknown*, 2017. URL <http://cs.jhu.edu/~jason/papers/mei+eisner.nips17.pdf>.

OpenAI, Achiam, J., Adler, S., Agarwal, S., Ahmad, L., Akkaya, I., Aleman, F. L., Almeida, D., Altenschmidt, J., Altman, S., Anadkat, S., Avila, R., Babuschkin, I., Balaji, S., Balcom, V., Baltescu, P., Bao, H., Bavarian, M., Belgum, J., Bello, I., Berdine, J., Bernadett-Shapiro, G., Berner, C., Bogdonoff, L., Boiko, O., Boyd, M., Brakman, A.-L., Brockman, G., Brooks, T., Brundage, M., Button, K., Cai, T., Campbell, R., Cann, A., Carey, B., Carlson, C., Carmichael, R., Chan, B., Chang, C., Chantzis, F., Chen, D., Chen, S., Chen, R., Chen, J., Chen, M., Chess, B., Cho, C., Chu, C., Chung, H. W., Cummings, D., Currier, J., Dai, Y., Decareaux, C., Degry, T., Deutsch, N., Deville, D., Dhar, A., Dohan, D., Dowling, S., Dunning, S., Ecoffet, A., Eleti, A., Eloundou, T., Farhi, D., Fedus, L., Felix, N., Fishman, S. P., Forte, J., Fulford, I., Gao, L., Georges, E., Gibson, C., Goel, V., Gogineni, T., Goh, G., Gontijo-Lopes, R., Gordon, J., Grafstein, M., Gray, S., Greene, R., Gross, J., Gu, S. S., Guo, Y., Hallacy, C., Han, J., Harris, J., He, Y., Heaton, M., Heidecke, J., Hesse, C., Hickey, A., Hickey, W., Hoeschele, P., Houghton, B., Hsu, K., Hu, S., Hu, X., Huizinga, J., Jain, S., Jain, S., Jang, J., Jiang, A., Jiang, R., Jin, H., Jin, D., Jomoto, S., Jonn, B., Jun, H., Kaftan, T., Łukasz Kaiser, Kamali, A., Kanitscheider, I., Keskar, N. S., Khan, T., Kilpatrick, L., Kim, J. W., Kim, C., Kim, Y., Kirchner, J. H., Kiros, J., Knight, M., Kokotajlo, D., Łukasz Kondraciuk, Kondrich, A., Konstantinidis, A., Kosic, K., Krueger, G., Kuo, V., Lampe, M., Lan, I., Lee, T., Leike, J., Leung, J., Levy, D., Li, C. M., Lim, R., Lin, M., Lin, S., Litwin, M., Lopez, T., Lowe, R., Lue, P., Makanju, A., Malfacini, K., Manning, S., Markov, T., Markovski, Y., Martin, B., Mayer, K., Mayne, A., McGrew, B., McKinney, S. M., McLeavey, C., McMillan, P., McNeil, J., Medina, D., Mehta, A., Menick, J., Metz, L., Mishchenko, A., Mishkin, P., Monaco, V., Morikawa, E., Mossing, D., Mu, T., Murati, M., Murk, O., Mély, D., Nair, A., Nakano, R., Nayak, R., Neelakantan, A., Ngo, R., Noh, H., Ouyang, L., O’Keefe, C., Pachocki, J., Paino, A., Palermo, J., Pantuliano, A., Parascandolo,

G., Parish, J., Parparita, E., Passos, A., Pavlov, M., Peng, A., Perelman, A., de Avila Belbute Peres, F., Petrov, M., de Oliveira Pinto, H. P., Michael, Pokorny, Pokrass, M., Pong, V. H., Powell, T., Power, A., Power, B., Proehl, E., Puri, R., Radford, A., Rae, J., Ramesh, A., Raymond, C., Real, F., Rimbach, K., Ross, C., Rotstod, B., Roussez, H., Ryder, N., Saltarelli, M., Sanders, T., Santurkar, S., Sastry, G., Schmidt, H., Schnurr, D., Schulman, J., Selsam, D., Sheppard, K., Sherbakov, T., Shieh, J., Shoker, S., Shyam, P., Sidor, S., Sigler, E., Simens, M., Sitkin, J., Slama, K., Sohl, I., Sokolowsky, B., Song, Y., Staudacher, N., Such, F. P., Summers, N., Sutskever, I., Tang, J., Tezak, N., Thompson, M. B., Tillet, P., Tootoonchian, A., Tseng, E., Tuggle, P., Turley, N., Tworek, J., Uribe, J. F. C., Vallone, A., Vijayvergiya, A., Voss, C., Wainwright, C., Wang, J. J., Wang, A., Wang, B., Ward, J., Wei, J., Weinmann, C., Welihinda, A., Welinder, P., Weng, J., Weng, L., Wiethoff, M., Willner, D., Winter, C., Wolrich, S., Wong, H., Workman, L., Wu, S., Wu, J., Wu, M., Xiao, K., Xu, T., Yoo, S., Yu, K., Yuan, Q., Zaremba, W., Zellers, R., Zhang, C., Zhang, M., Zhao, S., Zheng, T., Zhuang, J., Zhuk, W., and Zoph, B. Gpt-4 technical report, 2024. URL <https://arxiv.org/abs/2303.08774>.

Panayotov, V., Chen, G., Povey, D., and Khudanpur, S. Librispeech: an asr corpus based on public domain audio books. In *Acoustics, Speech and Signal Processing (ICASSP), 2015 IEEE International Conference on*, pp. 5206–5210. IEEE, 2015.

Patil, S. G., Zhang, T., Wang, X., and Gonzalez, J. E. Gorilla: Large language model connected with massive APIs. In *The Thirty-eighth Annual Conference on Neural Information Processing Systems*, 2024. URL <https://openreview.net/forum?id=tBRNC6YemY>.

Sakshi, S., Tyagi, U., Kumar, S., Seth, A., Selvakumar, R., Nieto, O., Duraiswami, R., Ghosh, S., and Manocha, D. MMAU: A massive multi-task audio understanding and reasoning benchmark. In *The Thirteenth International Conference on Learning Representations*, 2025. URL <https://openreview.net/forum?id=TeVAZXr3yv>.

Schick, T., Dwivedi-Yu, J., Dessi, R., Raileanu, R., Lomeli, M., Hambro, E., Zettlemoyer, L., Cancedda, N., and Scialom, T. Toolformer: Language models can teach themselves to use tools. In Oh, A., Naumann, T., Globerson, A., Saenko, K., Hardt, M., and Levine, S. (eds.), *Advances in Neural Information Processing Systems*, volume 36, pp. 68539–68551. Curran Associates, Inc., 2023. URL [https://proceedings.neurips.cc/paper\\_files/paper/2023/file/d842425e4bf79ba039352da0f658a906-Paper-Conference.pdf](https://proceedings.neurips.cc/paper_files/paper/2023/file/d842425e4bf79ba039352da0f658a906-Paper-Conference.pdf).

Stöter, F.-R., Chakrabarty, S., Edler, B., and Habets, E. A. P. Countnet: Estimating the number of concurrent speakers using supervised learning. *IEEE/ACM Transactions on Audio, Speech, and Language Processing*, 27(2):268–282, 2019. doi: 10.1109/TASLP.2018.2877892.

Team, G., Anil, R., Alayrac, J., Yu, J., Soricut, R., Schalkwyk, J., and .... Gemini: A family of highly capable multimodal models. *arXiv preprint arXiv:2312.11805*, 2023.

Wang, C., Luo, W., Dong, S., Xuan, X., Li, Z., Ma, L., and Gao, S. Mllm-tool: A multimodal large language model for tool agent learning. In *2025 IEEE/CVF Winter Conference on Applications of Computer Vision (WACV)*, pp. 6678–6687, 2025a. doi: 10.1109/WACV61041.2025.00650.

Wang, T., Cheng, C., Wang, L., Chen, S., and Zhao, W. Himtok: Learning hierarchical mask tokens for image segmentation with large multimodal model, 2025b. URL <https://arxiv.org/abs/2503.13026>.

Wang, Y., Xu, B., Yue, Z., Xiao, Z., Wang, Z., Zhang, L., Yang, D., Wang, W., and Jin, Q. Time-r1: Post-training large vision language model for temporal video grounding. 2025c. URL <https://api.semanticscholar.org/CorpusID:277103988>.

Wijngaard, G., Formisano, E., Esposito, M., and Dumontier, M. Audsemthinker: Enhancing audio-language models through reasoning over semantics of sound, 2025. URL <https://arxiv.org/abs/2505.14142>.

Xie, Z., Lin, M., Liu, Z., Wu, P., Yan, S., and Miao, C. Audio-reasoner: Improving reasoning capability in large audio language models, 2025. URL <https://arxiv.org/abs/2503.02318>.

Xu, J., Guo, Z., He, J., Hu, H., He, T., Bai, S., Chen, K., Wang, J., Fan, Y., Dang, K., Zhang, B., Wang, X., Chu, Y., and Lin, J. Qwen2.5-omni technical report, 2025a. URL <https://arxiv.org/abs/2503.20215>.

Xu, J., Guo, Z., Hu, H., Chu, Y., Wang, X., He, J., Wang, Y., Shi, X., He, T., Zhu, X., Lv, Y., Wang, Y., Guo, D., Wang, H., Ma, L., Zhang, P., Zhang, X., Hao, H., Guo, Z., Yang, B., Zhang, B., Ma, Z., Wei, X., Bai, S., Chen, K., Liu, X., Wang, P., Yang, M., Liu, D., Ren, X., Zheng, B., Men, R., Zhou, F., Yu, B., Yang, J., Yu, L., Zhou, J., and Lin, J. Qwen3-omni: A single multimodal model for text, image, audio, and video. *arXiv preprint arXiv:2509.17765*, 2025b.

## A. Appendix

### A.1. Hyperparameters

Table 6. Hyperparameter settings and training configurations.

Hyperparameter	Value
Learning Rate	$1 \times 10^{-6}$
Effective Batch Size	8
Optimizer	AdamW
Adam $\beta_1, \beta_2$	0.9, 0.999 (default)
Weight Decay	0.01 (default)
<b>Training Epochs</b>	
Qwen2.5-Omni 3B (All datasets)	3
Qwen2.5-Omni 7B (General)	6
Librispeech (All sizes, except below)	3
Librispeech 7B (Multi-timestamp task)	6
<b>Checkpoint Selection Metric</b>	
Librispeech	Max 20ms Accuracy
Libricount / AudioSet	Max 40ms Accuracy

### A.2. Dataset Examples

We provide examples of prompts from the datasets and the expected model outputs from token generation.

#### A.2.1. LIBRISPEECH

- **Prompt:** When does the 1st occurrence of the word 'much' occur?
- **Target Output:**

```
```json
[
    {"word": "much", "start": 0.63}
]
```
```

#### A.2.2. LIBRICOUNT

- **Prompt:** When does the 3rd speaker start speaking?
- **Target Output:**

```
```json
[
    {"speaker": "3", "start": 3.744}
]
```
```

#### A.2.3. AUDIOSET

- **Prompt:** When does the 2nd occurrence of the event 'Male singing' occur?
- **Target Output:**

```
```json
[
    {"event": "Male singing", "start": 1.821}
]
```

```

#### A.2.4. LIBRISPEECH (MULTI-TIMESTAMP INFERENCE)

- **Prompt:**

Transcript:  
mister verloc was fully responsive now  
Based on the transcript, output the timestamps for every word

- **Target Output:**

```
```json
[0.21, 0.49, 0.85, 1.04, 1.27, 1.86]
```

```